Canadian Geotechnical Journal
Revue canadienne de géotechnique

In-situ monitoring of frost heave pressure during cross passage construction using ground freezing method

Journal:	*Canadian Geotechnical Journal*
Manuscript ID	cgj-2014-0486.R2
Manuscript Type:	Article
Date Submitted by the Author:	07-Aug-2015
Complete List of Authors:	HAN, Lei; Shanghai Jiao Tong University, Department of Civil Engineering and State Key Laboratory of Ocean Engineering YE, Guanlin; Shanghai Jiao Tong University, Department of Civil Engineering LI, Yuan-hai; China University of Mining and Technology, State Key Laboratory for Geomechanics & Deep Underground Engineering XIA, Xiao-he; Shanghai Jiao Tong University, Department of Civil Engineering and State Key Laboratory of Ocean Engineering Wang, Jianhua; Shanghai Jiao Tong University, Department of Civil Engineering and State Key Laboratory of Ocean Engineering
Keyword:	in-situ monitoring, frost heave pressure, shield tunnel, ground freezing method, water migration

In-situ monitoring of frost heave pressure during cross passage construction using ground freezing method

Lei HAN
Department of Civil Engineering and State Key Laboratory of Ocean Engineering,
Shanghai Jiao Tong University, Shanghai, 200240, China
hanleiwell@163.com

Guan-lin YE
(CORRESPONDING AUTHOR)
Department of Civil Engineering and State Key Laboratory of Ocean Engineering,
Shanghai Jiao Tong University, Shanghai, 200240, China
ygl@sjtu.edu.cn

Yuan-hai LI
State Key Laboratory for Geomechanics & Deep Underground Engineering, China
University of Mining and Technology, Xuzhou, 221116, China
lyh@cumt.edu.cn

Xiao-he XIA
Department of Civil Engineering and State Key Laboratory of Ocean Engineering,
Shanghai Jiao Tong University, Shanghai, 200240, China
xhxia@sjtu.edu.cn

Jian-hua WANG
Department of Civil Engineering and State Key Laboratory of Ocean Engineering,
Shanghai Jiao Tong University, Shanghai, 200240, China
wjh417@sjtu.edu.cn

Abstract

The artificial ground freezing method has the dual effect of ground reinforcement and waterproof sealing, and the frozen curtain can be designed flexibly. It is widely used in the construction of cross passages for shield tunnels in soft ground with high groundwater levels. However, due to the lack of in-situ monitoring data, it remains difficult to determine the frost heave pressure acting upon a tunnel. In this study, based on the use of an anti-freezing pad-type earth pressure gauge, in-situ monitoring was carried out to measure the frost heave pressure acting upon tunnel segments during the construction of cross passages for the Shanghai Yangtze River Tunnel. The monitoring results show that the earth pressure acting upon the tunnel could decrease dramatically during freezing, and this kind of decrease can take place suddenly and unpredictably, which can be illustrated using the finite element method. The maximum measured frost heave pressure during freezing and cross passage excavation was approximately 0.2MPa, which was much smaller than the predicted value. Combining the distribution of temperature in the ground and construction countermeasures, the observed phenomena are mainly related to three factors: water migration during the freezing process, the tunnel-ground interaction and the countermeasure of pressure release holes. The tunnel showed a horizontal extension deformation, which was consistent with the releasing frost heave pressure acting upon it.

Keywords: in-situ monitoring, frost heave pressure, shield tunnel, ground freezing method, water migration

1. Introduction

The artificial ground freezing method is widely used in geotechnical engineering. It can be adapted to engineering in complex geological and hydrological conditions with almost no pollution (Whittaker and Frith 1990; Konrad 2002; Brown, 2004; Yang et al. 2006; Casini et al., 2014), especially in soft ground with high water content. This method has the dual effect of ground reinforcement and waterproof sealing, as it can form a coherent and closed waterproof curtain, which has high strength, high stiffness and practically zero permeability (Andersland and Ladanyi 2004; Ou et al. 2009). It has been successfully used in many cross passage construction projects (Biggart and Sternath 1996; Haß and Schäfers 2005; Crippa and Manassero 2006; Zhang et al. 2011; Ye et al. 2013). Statistics show that the artificial ground freezing method has been used in almost all cross passages in metro tunnels and cross-river road tunnels in Shanghai (Xiao 2007), making it an invaluable technique in the construction of cross passages.

The mechanism of frost heave is complicated and many researchers have developed models to analyse the heat and mass transfer, and the phase change mechanics of frost heave (Harlan 1973; Taylor and Luthin 1978; Gilpin 1980; Guymon et al. 1980; Konrad and Morgenstern 1980, 1984; O'Neill and Miller 1985; Shen and Ladanyi 1987; Fremond and Mikkola 1991; Nixon 1991; Konrad and Duquennoi 1993; Selvadurai et al. 1999; Coussy 2005; Sheng et al. 2013, etc.). Early in the 17th century people had noticed the frost heave phenomenon. Not until the 20th century did researchers have a correct understanding of the mechanism of frost heave, in which water migration is the main reason for soil frost heave (Miller 1972; Harlan 1973; Gilpin 1980; Gray and Granger 1986; Nakano and Tice 1990; Konrad 2002; Talamucci 2003, etc.). Frost heave includes in-situ heave and segregation heave. In-situ heave is caused by in-situ water freezing, resulting in a volume increase of 9%. Segregation heave is caused by the water migrating to the freezing front causing a 1.09 times increase in volume (Konrad and Morgenstern 1980; Yang et al. 2006). Segregation heave is the main component of soil frost heave. A soft soil layer rich in water content will produce a large volume expansion, resulting in a large frost heave pressure. Frost heave pressure has frequently caused deformation or destruction to neighboring structures in cold regions (Lai et al., 1998; Palmer and Williams, 2003). Therefore, attention should be paid to the frost heave pressure acting upon the tunnel segments during the construction of cross passages using the artificial ground freezing method.

Some in-situ monitoring has been carried out during the construction of cross passages. This involved disk type earth pressure transducers being mounted onto a steel pipe and inserted into a borehole in the prescribed frozen zone, as shown in Fig. 1. With this method, the maximum measured frost heave pressure was about 1.5 MPa during the construction of a cross passage for the Shanghai Dalian Road Tunnel (Yue et al., 2006); the maximum pressure was 1.8 MPa in a cross passage construction for the Nanjing Metro tunnel (Qiao et al., 2003). Such a large pressure may have imposed a safety threat to the tunnels. However, the frost heave pressure measured by the aforementioned method (Fig.1) is the pressure within the frozen soil, not the interaction pressure between the frozen soil and the tunnel structure. Until now, little literature has been available on monitoring the frost heave pressure acting upon tunnel segments.

In this study, a new type of anti-freezing earth pressure gauge was applied to measure the frost heave pressure acting upon the tunnel segments during the cross passage construction for the Shanghai Yangtze River Tunnel. The deformation of the tunnels and the temperature changes in the frozen curtain were monitored at the same time. The monitoring data is analysed carefully with reference to the construction information of the cross passages.

2. Cross passage construction with artificial ground freezing method

The cross passages of shield tunnels are usually built in combination with a drainage sump, and they play an important part in the catchment, drainage and connection of the two tunnels, and provide emergency escape routes for passenger evacuation, and access routes for rescue services (e.g., Murray, 1997). Before cross passage excavation, the surrounding soil must be reinforced. There are two construction stages in cross passage construction using the artificial ground freezing method. In the first stage, the soil surrounding the cross passage is frozen to form a reinforced and waterproof curtain. In this stage, freezing pipes are installed into the horizontal and inclined bored holes from the main tunnel, as shown in Fig. 2. Then the surrounding soil is frozen by circulating the cryogenic refrigerant through the freezing pipes. In the second stage, the cross passage and drainage sump are constructed using the mining method, as shown in Photo 1.

3. Project profile

The Shanghai Yangtze River Tunnel is one of the largest shield tunnels in the world. It is a twin-tube shield tunnel with a total length of 8.95km. The outer and inner diameters are 15m and 13.7m, respectively. Each ring of the tunnel is composed of 10 reinforced concrete segments with a thickness of 0.65m and a width of 2m. Steel segments are used at the positions of the cross passages, with the same thickness and width as the concrete ones. The clear distance between the two tubes is approximately 15m. A total of eight cross passages were constructed, each with a length of approximately 15m. Sectional and plan views of a cross passage are shown in Fig.3. The outer and inner diameters of the ring of frozen soil are 9.34m and 3.94m, respectively, and its thickness is 2.7m. The design value for the average frozen temperature of the frozen ring was -15°C.

The ground profile is shown in Fig.3. The cross passage is located in the 5-3 silty clay layer. The geotechnical and thermal properties of the 5-3 silty clay are shown in Table 1, and its mechanical properties at different temperatures (-8°C, -15°C, -20°C and -25°C) are shown in Table 2. Unidirectional freezing tests were conducted on the 5-3 silty clay to obtain the frost heave pressure and the frost heave ratio under the closed system. It was found that the average frost heave pressure and frost heave ratio (defined as the ratio of volume increment to initial volume of a specimen) of 5-3 silty clay were 0.71MPa and 6.35%, respectively. The overall ground profile in the

Shanghai area can be referred to in Wu et al. (2014).

4. In-situ monitoring method

4.1 Earth pressure gauge

A pad-type earth pressure gauge (Hashimoto et al. 1993, 2002a, 2002b) with a large diaphragm of 750mm×450mm was used to measure the frost heave pressure acting upon the tunnel segments, as shown in Photo 2. The inside of the stainless cell is filled with incompressible liquid. The liquid pressure is measured by a vibrating wire type pressure sensor. Compared with the conventional 120mm diameter disc-type earth pressure gauge, the pad-type earth pressure gauge has the following advantages: (1) The pressure diaphragm is flexible, so that it can be mounted on the outer surface of the circular shield tunnel segments smoothly. (2) The maximum thickness of the pressure plate is less than 6mm, so it will not damage the tail brush, and can avoid any soil arching effect during measurement. (3) The large pressure diaphragm can obtain a more accurate average earth pressure than a conventional 120mm diameter disc-type pressure gauge. (4) The gauge is made of stainless steel, which has excellent long-term durability. With these advantages, the pad-type earth pressure gauge is suitable for measuring the earth pressure on the tunnel segments. In this study, in order to measure the earth pressure under cold conditions, an anti-freezing liquid was used to fill the pressure cell. It was confirmed through calibration that both the linearity error and the hysteresis error were less than 1% of the full measurement range.

The installation method for the pad-type earth pressure gauge is given in Fig.4. The pressure diaphragm is fixed to the outer surface of the segment and the pressure sensor and cable are placed in the existing holes in the segment. Each pressure sensor is fixed with a temperature sensor to measure the temperature at the pad-type earth pressure gauge location. Then the holes are sealed with cured epoxy resin. This kind of sealing has been proven to be effective under water pressure of 1MPa. The earth pressure gauges before and after the installation are shown in Photo 2. The data was collected by a universal automatic data logging instrument.

4.2 Layout of Measuring Points

The layout of the frost heave pressure measuring points on the steel segments was determined based on the following considerations: (1) the frost heave pressure should be measured around the cross passage at different locations, in order to obtain the loading distribution. (2) One earth pressure gauge was installed on one segment, reducing the risk of it being damaged. Accordingly, five earth pressure gauges were installed on 5 segments at Ring No. 2057-2060 of the up line tunnel, as shown in Fig.5.

In order to obtain the temperature distribution and the development of the freezing curtain, thermocouple sensors were also installed in 6 measuring holes (T1-T6), as shown in Fig.5 (b).

5. Cross passage construction and in-situ monitoring

The ground freezing began on May 26th, 2008 (Photo 3) and excavation began on August 10th by the mining method. The concrete spraying began on August 20, the waterproof sheet was laid on August 22nd, and the inner lining was constructed on August 26th. Freezing stopped on September 1st.

The segments of rings No. 2057-2060 were assembled on January 7th, 2008. The measuring data was recorded immediately after the assembly. The data before the segments passed the tail brush were taken as the initial reference values. After measuring continuously for two days, the final monitoring values were compared with the theoretical earth pressure to confirm the validity (Ye et al. 2010). The monitoring was then paused.

Measurement was restarted on May 23rd, 3 days before the freezing works. Manual measurement was carried out from June 2nd to June 12th, once per hour in the daytime. Automatic measurement was conducted from June 13th to September 19th 2008, with a time interval of 2 hours. In-situ monitoring covered the entire cross passage construction process, and a complete data record was obtained.

6. Analysis of monitoring data

6.1 Verification of pad-type earth pressure gauge under cold conditions

In order to verify the applicability of the pressure gauge at low temperatures, a loading test was carried out in a frozen chamber at -35°C with two different loads of 0.98kN and 1.47kN. Fig. 6 shows the relationship between measured pressures and applied loads at the temperature of -35°C. The pressure was obtained by subtracting the initial value (0kN load at 20°C) from the measured values at -35°C. It can be seen that the anti-freezing pad-type earth pressure gauge can output stable pressure values separately with two different applied loads at a low temperature. By applying a linear curve-fitting between applied loads and measured pressures, a shift of 1.697kPa that caused by the change of temperature from 20°C to -35°C can be obtained. This shift is relatively small by comparing with the overburden loads, therefore it can be ignored. At the same time, the measured pressure increment was 1.455kPa (=6.056- 4.601) at -35°C, with a load increment of 0.49kN (=1.47-0.98). Compared with the increment of 1.452kPa (=4.356-2.904) at 20°C, the pressure gauges maintained the same precision under low temperatures as at room temperatures. Therefore, the pressure gauge can output stable pressure values at low temperatures and the monitoring values are reliable.

6.2 Change in measured earth pressure and temperature

Fig. 7 shows the change in five measured values of earth pressure and temperatures during the construction of the cross passages. The changes in measured earth pressure can be divided into the following 6 phases:

(1) Early stage of positive freezing (from the beginning of the freezing process to the 14th day): the earth pressure of gauges 20121-20123, which were located on the top and bottom of the frozen ring, showed an increasing trend, while the earth pressure of gauges 20124 and 20125, which were located near the horizontal spring line, decreased at first and then increased. The maximum increment in gauge 20123

was 186kPa. The temperatures at 5 pressure gauges dropped quickly, and those at 20124 and 20125 were lower than zero degrees Celsius.

(2) Middle stage of positive freezing (14th-30th day): the earth pressure of gauges 20123-20125 decreased to almost 0kPa, while the earth pressure of 20121 and 20122 remained stable. All 5 temperatures dropped gently to below zero degrees Celsius.

(3) Late stage of positive freezing (30th-75th day): the earth pressure of gauge 20121 suddenly reduced, and the other four gauges remained stable. Before the excavation, with the exception of 20122, the earth pressures of the gauges reduced to almost 0kPa. The temperatures kept constant except for a small jump around the 55th day.

(4) Cross passage excavation (duration about 10 days): all measured values of earth pressure and temperature changed slightly.

(5) Structural construction of cross passage (duration about 10 days): the earth pressures of gauges 20121 and 20124 increased, while that of the other three gauges remained unchanged. The temperatures increased to positive values.

(6) From the end of the freezing process to September 19th (duration about 20 days): all measured points changed considerably. Except for gauge 20122, the remaining four points first rose to the load level before freezing and then decreased gradually, while 20122 only showed a gradually decreasing trend.

6.3 Temperature distribution along T2 measuring hole

The temperature distribution along the T2 measuring hole (Fig. 5) at different times during the freezing process is shown in Fig.8. The temperature dropped quickly in the early stage of freezing, especially at the position near the middle part of the cross passage. The minimum temperature in the middle section of the cross passage reached about -25°C. The temperatures of the soil adjacent to the tunnels dropped at a slower rate than those in the central part of the cross passage. The lowest temperature was about -11°C at the outer surface of the segment, while those in the middle of the cross passage reached -25°C. This was due to the heat dissipation from the tunnel segments (Lai et al., 2005; Ye et al., 2013).

6.4 Mechanism of frost heave pressure acting upon segments during cross passage construction

Combining the changes from the earth pressure gauges (Fig.7(a)) and the temperature changes (Fig.7(b)), as well as the temperature distribution along the T2 measuring hole (Fig.8), the mechanism of the frost heave pressure acting upon the segments during the cross passage construction is as follows: (1) The temperature of the soil drops quickly in the early stage of freezing. The ground water in the soil begins to freeze and expand, resulting in a heaving pressure acting on the tunnel. (2) When a continuous freezing zone is formed, the frozen soil has a high strength and almost stops expanding. The contact between the frozen soil and the segments was practically the same as if they formed a rigid body together. It is well known that this type of contact is very sensitive, to even small temperature changes, or to an unevenness of the frozen soil surface. Several factors may lead to a steep drop or rise in the pressure on the tunnel, such as a slight deformation of the tunnel or of the pressure cell of the pad-type earth pressure gauge, which will lead to an instantaneous separation or contact between stiff frozen soil and the tunnel; or non-uniform deformation of frozen soil and unfrozen soil along the contact surface, which is illustrated using FEM in the next section. (3) Due to construction disturbance and temperature changes during the cross passage construction, the frost heave pressure becomes complex. After the freezing process is stopped, the frozen soil thaws gradually, the soil becomes soft and the contact between soil and tunnel resumes.

6.5 Numerical explanation for rapid reduction in frost heave pressure during freezing

(1) FEM model

A finite element code with a thermo-mechanical coupled feature was applied to analyse the rapid reduction in frost heave pressure during freezing. Fig. 9 shows the two-dimensional FEM model. The displacement boundary is set up as follows: the left side is fixed horizontally, the lower boundary is fixed vertically, and the right side is a symmetry boundary. Contact elements are used to represent the contact and sliding between tunnel and soils. The FEM model includes 4863 elements and 4983 nodes.

(2) Material properties and parameters

A Mohr Coulomb type soil plasticity constitutive model was used during the analysis. The material properties and parameters of the soils are shown in Table 3. The elastic modulus and Poisson's ratio of concrete are 3×10^4 MPa and 0.2, respectively. The expansion of frozen soil is assumed to be linear. Since the frost heave ratio of 5-3 silty clays is 6.35% at -25°C degrees Celsius (described in Chapter 3), its coefficient of linear expansion is $(\sqrt[3]{1+6.35\%}-1)/25$ =0.08%/°C. The expansion only takes place when the temperature is lower than 0°C. Because the freezing front mainly developed perpendicularly to the freezing pipe, without loss of generality, it was assumed that the vertical and horizontal linear expansion coefficients are 0.08%/°C and 0.008%/°C, respectively. In the analysis, the first step was the gravity stress calculation. The second step was the tunnel excavation. In the third step, the prescribed frozen ring in Fig. 9 was subjected to a decrease in temperature until it reached the final value in Fig. 10.

(3) Calculation results

Fig. 11 shows the horizontal displacement increments of the tunnel and the soils in the frozen zone. The increments are obtained by subtracting the displacements before freezing from those after freezing. It can be seen that in the cross passage region, the horizontal displacements of the tunnel and the soil were almost the same. However, in the frozen region, the horizontal displacements of the tunnel were greater than those of the frozen soil. This suggests that the tunnel and the frozen soil were detached from each other in the frozen zone, leading to a drop of frost heave pressure acting upon tunnel. Fig. 12 shows the distribution of the values of σ_x (horizontal stress) which are obtained by subtracting the values of σ_x before freezing from those after freezing. The mechanism for the detachment can be explained as follows: when the frozen ring expanded along its radial direction, the enclosed unfrozen soils were squeezed then pushed against the tunnel. Fig. 12 shows that the values of σ_x for unfrozen soils increased, while those of frozen soils decreased, which indicates that the pressures on the tunnel due to pressure from the unfrozen soil were greater than those from the frozen soil. As a result, the tunnel and frozen soils separated. It should be pointed out that this simulation needs to be verified by in-situ monitoring or laboratory model testing.

6.6 Discussion on smaller than expected frost heave pressure upon segments

Fig. 13 shows the frost heave pressures during the cross passage construction. Fig. 13(a) shows the values of five measuring points at different stages. Fig. 13(b) shows the maximum frost heave pressures, which are obtained by subtracting the initial earth pressure just before freezing from the earth pressure in the initial freezing stage (maximum pressure). It can be seen that the maximum frost heave pressure was 186kPa, which is much lower than that inside the frozen soil measured by previous studies (Yue et al. 2006; Qiao et al. 2003). Three reasons can be given for this difference.

(1) It is generally well known that frost heave is not only caused by freezing of local ground water but also by water flow to a freezing front where it forms ice lenses (Gray and Granger 1986; Konrad 1994, 2002, 2008). According to the temperature distribution along the T2 measuring hole at different time during the freezing process (Fig.8), due to heat dissipating from the tunnel segments, the temperature of the soil adjacent to the tunnels fell more slowly than the soil in the central part of the cross passage. Therefore the water in the middle froze earlier than that near the tunnels, and

the water near the segments appears to have migrated to the central part, as shown in Fig.14. The frost heave adjacent to the segments reduced, resulting in a smaller frost heave pressure than that in the central part.

(2) The ground reaction pressure to the tunnel is relatively small in soft ground. Therefore the tunnel is prone to move laterally under the frost heave pressure, which may decrease the pressure acting on tunnel segments.

(3) Countermeasures were taken to reduce the frost heave pressure during construction. Two pressure relief holes were installed in the steel segments to release the earth pressure. They were opened from time to time during the ground freezing process. Studies by Ooi et al. (2002) also confirmed the possibility of relief pressure to reduce the frost heave pressure.

6.7 Cross-sectional deformation of tunnel

The cross-sectional deformation of the tunnel was measured, in order to observe the influence of cross passage construction on the tunnel structure. The timeline of inner deformation is shown in Fig.15. In the figure, "+" represents extension, and "-" represents shrinkage. It can be seen from Fig.15 that the deformation changed slowly in the early stage of freezing, and remained almost stable after that. Horizontal deformation showed extension, and vertical deformation showed shrinkage. This kind of deformation indicates that the horizontal earth pressure decreased during freezing. In other words, the trend of deformation coincided with that of the measured earth pressures. The range of deformation is within ±5mm.

7. Conclusions

In-situ monitoring of the frost heave pressure acting upon a shield tunnel during cross passage construction was carried out in the Shanghai Yangtze River Tunnel. Through a careful analysis of the monitoring data, the following conclusions can be drawn:

(1) The pad-type earth pressure gauge, which can work at low temperatures, can be used to measure the frost heave pressure acting upon a shield tunnel during the construction of cross passages using the artificial ground freezing method.

(2) In-situ monitoring showed that during positive freezing, the earth pressure acting upon the tunnels may decrease dramatically, and this kind of decrease takes place suddenly and unpredictably. After the freezing process stopped, the earth pressure showed an increasing trend toward the load level before freezing. Finite element analysis showed that due to the squeezing effect of the frozen ring on the enclosed soft soils, the tunnel and frozen soils detached from each other, leading to a drop in frost heave pressure upon the tunnel.

(3) The maximum measured increment of earth pressure during the cross passage construction was about 0.2MPa, which was smaller than the expected value. In addition to the water migrating during the freezing process, it also migrated due to the tunnel-ground interactions and the countermeasure of the pressure relief holes that were set up to release the frost heave pressure.

(4) The measured cross-sectional deformation of the tunnel showed a trend of

horizontal extension, which was consistent with the change in measured earth pressure upon the tunnel.

Acknowledgements

The authors would like to thank Mr. Ji-yun Wang of STEC Co. Ltd. for the invaluable discussions, and thank Prof. Xiang-dong Hu of Tongji University for providing the in-situ measured temperature data. The support of the National Nature Science Foundation of China (Grant No. 41372284 and 51174197) and the Science and Technology Commission of Shanghai Municipality (Funding No. 14231200602) are also greatly appreciated.

References

Andersland, O.B., Ladanyi, B. 2004. Frozen ground engineering. John Wiley & Sons.

Biggart, A. R., Sternath, R. 1996. Storebælt eastern railway tunnel: construction. Proceedings of the ICE-Civil Engineering. Thomas Telford, 114(5), 20-39.

Brown, D.A. 2004. Hull waste water flow transfer tunnel: recovery of tunnel collapse by ground freezing. Proceedings of the ICE-Geotechnical Engineering, 157(2), 77–83.

Casini, F., Gens, A., Olivella, S., and Viggiani, G. M. 2014. Artificial ground freezing of a volcanic ash: laboratory tests and modelling. Environmental Geotechnics. http://dx.doi.org/10.1680/envgeo.14.00004

Coussy, O. 2005. Poromechanics of freezing materials. Journal of the Mechanics and

Physics of Solids, 53(8), 1689-1718.

Crippa, C., and Manassero, V. 2006. Artificial ground freezing at Sophiaspoor tunnel (The Netherlands) - Freezing parameters: Data acquisition and processing. GeoCongress 2006: Geotechnical Engineering in the Information Technology Age, Atlanta.

Fremond, M., and Mikkola, M. 1991. Thermomechanical modelling of freezing soil. Ground Freezing, 91, 17-24.

Gilpin, R.R. 1980. A model for the prediction of ice lensing and frost heave in soils. Water Resources Research, 16(5), 918-930.

Gray, D. M., and Granger, R. J. 1986. In situ measurements of moisture and salt movement in freezing soils. Canadian Journal of Earth Sciences, 23(5), 696-704.

Guymon, G., Berg, R., and Hromadka, T. 1980. A one-dimensional frost heaven model based upon simulation of simultaneous heat and water flux. Cold Regions Science and Technology, 3(2), 253– 263.

Harlan, R.L. 1973. Analysis of coupled heat-fluid transport in partially frozen soil. Water Resources Research, 9(5), 1314-1323.

Hashimoto, T., Brinkman, J., Konda, T., Kano, Y., and Feddema, A. 2002a. Simultaneous Backfill Grouting, Pressure Development in Construction Phase and in the Long-Term. Tunnelling. A Decade of Progress. GeoDelft 1995-2005, edited by H . van Lottum and A . Bezuijen, Taylor & Francis, 101–107.

Hashimoto, T., Nagaya, J., Konda, T., and Tamura, T. 2002b. Observation of lining pressure due to shield tunneling. Proceedings of 3rd International Symposium on

Geotechnical Aspects of Underground Construction in Soft Ground, IS-oulouse, 119-124.

Hashimoto, T., Yabe, K. and Yamane, S. 1993. Development of pad type earth pressure cell for shield segment. Proceedings of 28th Annual Report of JGS, Tokyo: Japan Geotechnical Society, 2055-2058.

Haß, H., Schäfers, P. 2005. Application of ground freezing for underground construction in soft ground. In Geotechnical Aspects of Underground Construction in Soft Ground: Proceedings of the 5th International Symposium TC28. Amsterdam, the Netherlands, 405-412.

Konrad, J.M. 1994. Sixteenth Canadian Geotechnical Colloquium: Frost heave in soils: concepts and engineering. Canadian Geotechnical Journal, 31(2), 223-245.

Konrad, J.M. 2002. Prediction of freezing-induced movements for an underground construction project in Japan. Canadian Geotechnical Journal, 39(6), 1231–1242.

Konrad, J. M. 2008. Freezing-induced water migration in compacted base-course materials. Canadian Geotechnical Journal, 45(7), 895–909.

Konrad, J.M., and Duquennoi, C. 1993. A model for water transport and ice lensing in freezing soils. Water Resources Research, 29(9), 3109-3124.

Konrad, J.M., and Morgenstern, N.R. 1980. A mechanistic theory of ice lens formation in fine-grained soils. Canadian Geotechnical Journal, 17(4), 473-486.

Konrad, J.M., Morgenstern, N.R., 1984. Frost heave prediction of chilled pipelines buried in unfrozen soils. Canadian Geotechnical Journal, 21(1), 100-115.

Lai, Y.M., Wu, Z.W., Zhu, Y.L., and Zhu, L.N. 1998. Nonlinear analysis for the coupled problem of temperature, seepage and stress fields in cold-region tunnels. Tunnelling and underground space technology, 13(4), 435-440.

Lai, Y. M., Zhang, X. F., Yu, W. B., Zhang, S-J., Liu, Z., and Jianzhang, X. 2005. Three-dimensional nonlinear analysis for the coupled problem of the heat transfer of the surrounding rock and the heat convection between the air and the surrounding rock in cold-region tunnel. Tunnelling and Underground Space Technology, 20(4), 323–332.

Miller, R.D. 1972. Freezing and heaving of saturated and unsaturated soils. Highway research record 393, 1-11.

Murray, M.J., and Eskesen, S.D. 1997. Design and construction of cross passages at the Størebælt Eastern Railway Tunnel. Tunnelling 97 Conference, 463-479.

Nakano, Y., and Tice, A.R. 1990. Transport of water due to a temperature gradient in unsaturated frozen clay. Cold Regions Science and Technology, 18(1), 57–75.

Nixon, J.F. 1991. Discrete ice lens theory for frost heave in soils. Canadian Geotechnical Journal, 28(6), 843-859.

O'Neill, K., and Miller, R.D. 1985. Exploration of a rigid ice model of frost heave. Water Resources Research, 21(3), 281-296.

Ooi, P. S., Walker, M. P., and Smith, J. D. 2002. Performance of a single-propped wall during excavation and during freezing of the retained soil. Computers and Geotechnics, 29(5), 387-409.

Ou, C.Y., Kao, C.C., and Chen, C.I. 2009. Performance and analysis of artificial ground freezing in the shield tunneling. Journal of GeoEngineering, 4(1), 29-40.

Palmer, A.C., and Williams, P.J. 2003. Frost heave and pipeline upheaval buckling. Canadian geotechnical journal, 40(5), 1033-1038.

Qiao, W. G., Li, D. Y., and Wu, X. Z. 2003. Survey analysis of freezing method applied to connected aisle in metro tunnel. Rock and Soil Mechanics, 24(4), 666-669. (in Chinese)

Selvadurai, A.P.S., Hu, J., and Konuk, I. 1999. Computational modelling of frost heave induced soil–pipeline interaction: I. Modelling of frost heave. Cold regions science and technology, 29(3), 215-228.

Shen, M., and Ladanyi, B. 1987. Modelling of coupled heat, moisture and stress field in freezing soil. Cold Regions Science and Technology, 14(3), 237-246.

Sheng, D.C., Zhang, S., Yu, Z.W., and Zhang, J.S. 2013. Assessing frost susceptibility of soils using PCHeave. Cold Regions Science and Technology, 95, 27-38.

Talamucci, F. 2003. Freezing processes in porous media: Formation of ice lenses, swelling of the soil. Mathematical and computer modelling, 37(5), 595-602.

Taylor, G.S., and Luthin, J.N. 1978. A model for coupled heat and moisture transfer during soil freezing. Canadian Geotechnical Journal, 15(4), 548-555.

Whittaker, B.N., and Frith, R.C. 1990. Tunnelling: design, stability and construction.

Wu, C.J., Ye, G.L., Zhang, L. L., Bishop, D., and Wang, J.H. 2014. Depositional environment and geotechnical properties of Shanghai clay: a comparison with Ariake and Bangkok clays. Bulletin of Engineering Geology and the Environment. Online. DOI:10.1007/s10064-014-0670-0

Xiao, Z. Y. 2007. Research on the Forming and Thawing of Frozen soil Walls by

Artificial Ground Freezing Method. PhD dissertation of Tongji University. Shanghai. (in Chinese)

Yang, P., Ke, J. M., Wang, J. G., Chow, Y. K., and Zhu, F. B. 2006. Numerical simulation of frost heave with coupled water freezing, temperature and stress fields in tunnel excavation. Computers and Geotechnics, 33(6), 330-340.

Ye, G.L., Wang, J.Y., Wang, J.H. and Qiao, B.Z. 2010. In-situ monitoring of construction loading acting upon segments of super large shield tunnel. Modern Tunnelling Technology, 47(5), 85-89. (in Chinese)

Ye, X.W., Ni, Y.Q., and Yin, J.H. 2013. Safety Monitoring of railway tunnel construction using FBG sensing technology. Advances in Structural Engineering, 16(8), 1401-1410.

Yue, F.T., Qiu, P. Y., Yang, G. X. and Shi, R.J. 2006. Design and practice of freezing method applied to connected aisle in tunnel under complex conditions. Chinese Journal of Geotechnical Engineering, 28(5), 660-663. (in Chinese)

Zhang, M., Wang, L.M., Wang, B.W., and Lin, H.B. 2011. Horizontal freezing study for cross passage of river-crossing tunnel. Sciences in Cold and Arid Regions, 3(4), 314-318.

TABLES

Table 1 Geotechnical and thermal properties of 5-3 silty clay.

Table 2 Mechanical properties of 5-3 silty clay under different temperatures (Tested with free water supply).

Table 3 Material properties and parameters of soils.

Table 1 Geotechnical and thermal properties of 5-3 silty clay

Moisture content (%)	Density (g/cm^3)	Permeability coefficient (cm/s)	Void ratio	Plastic limit (%)	Liquid limit (%)
35.1	1.78	1.99×10^{-6}	1.01	21.17	36.73
Salinity (‰)	Chloride ion concentration (‰)	Freezing temperature (°C)	Specific heat J/(g·K)	Thermal conductivity W/(m·K)	
				Unfrozen soil	Frozen soil
8.039	4.450	-2.1	1.65	1.42	1.74

Table 2 Mechanical properties of 5-3 silty clay under different temperatures (Tested with free water supply)

Mechanics property	Temperature			
	-8°C	-15°C	-20°C	-25°C
Uniaxial compressive strength (MPa)	3.07	3.95	5.16	6.60
Elastic modulus (MPa)	57.1	93.2	161.1	306.1
Poisson's ratio	0.259	0.242	0.217	0.206
Cohesion (MPa)	1.3	1.6	2.0	2.4
Internal friction angle (°)	22.6	23.4	23.8	25.4

Table 3 Material properties and parameters of soils

Soil layer	γ (kN/m^3)	Elastic modulus (MPa)	Poisson's ratio	c' (kPa)	φ' (°)
1-3 Clayey silt	18.4	6	0.3	10	26
4 Muddy caly	16.8	5	0.3	10	20
5-3 Silty clay	18.1	8	0.3	14	27

FIGURES

Fig. 1. Monitoring method for frost heave pressure with disk type pressure gauges mounted on a steel pipe in the frozen soil

Fig. 2. Schematic illustration of the arrangement of freezing pipes

Fig. 3. Sectional and plan view of cross passage for Shanghai Yangtze River Tunnel

Fig. 4. Installation method of pad-type earth pressure gauge

Fig. 5. Installation positions of 5 pad-type earth pressure gauges and temperature measuring holes

Fig. 6. Relationship between measured pressures and applied loads at the temperature of -35°C

Fig. 7. Timeline of measured earth pressures and temperatures

Fig. 8. Temperature distribution along T2 measuring hole at different times during the freezing process

Fig. 9. FEM model for analysing the drop-down of frost heave pressure during freezing

Fig. 10. Prescribed final temperatures in the frozen ring, used for thermal-mechanical coupled analysis

Fig. 11. Horizontal displacement increment of tunnel and soil in frozen zone between before and after freezing

Fig. 12. Distribution of σ_x, obtained by subtracting the values of σ_x before freezing from those after freezing

Fig. 13. Distribution of measured frost heave pressures upon the tunnel

Fig. 14. Illustration of water migration in the early stage of freezing

Fig. 15. Timeline of cross-sectional deformation of up line tunnel

Photo 1. Excavation of cross passage for Shanghai Yangtze River Tunnel by the mining method

Photo 2. Photos of earth pressure gauge before and after installation.

Photo 3. Photo taken in front of steel segments at the start of freezing

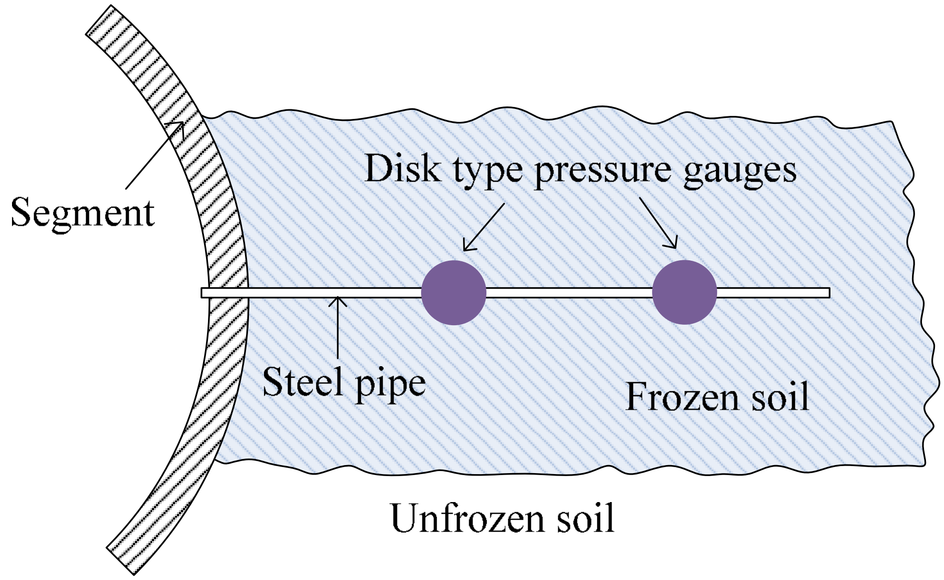

Fig. 1. Monitoring method for frost heave pressure with disk type pressure gauges mounted on a steel pipe in the frozen soil

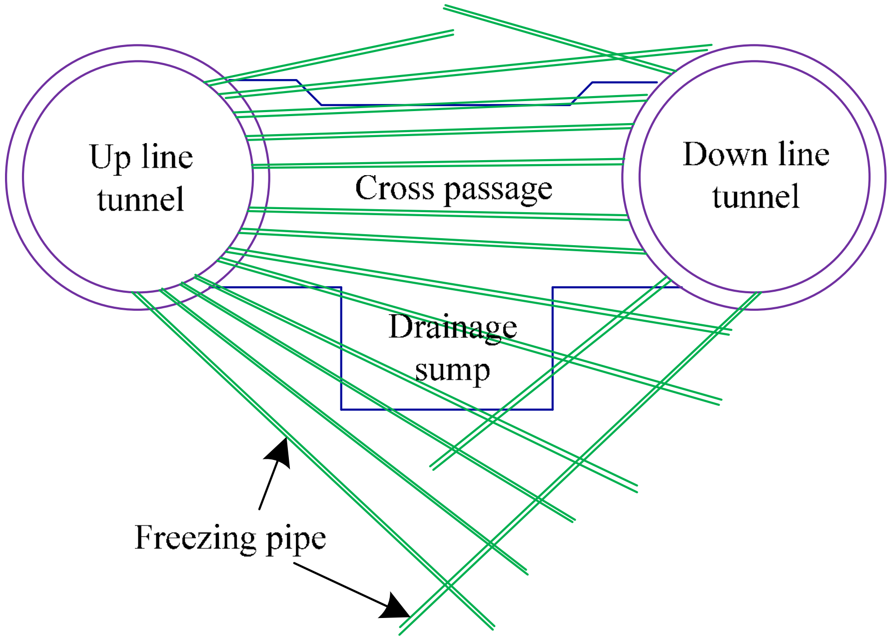

Fig. 2. Schematic illustration of the arrangement of freezing pipes

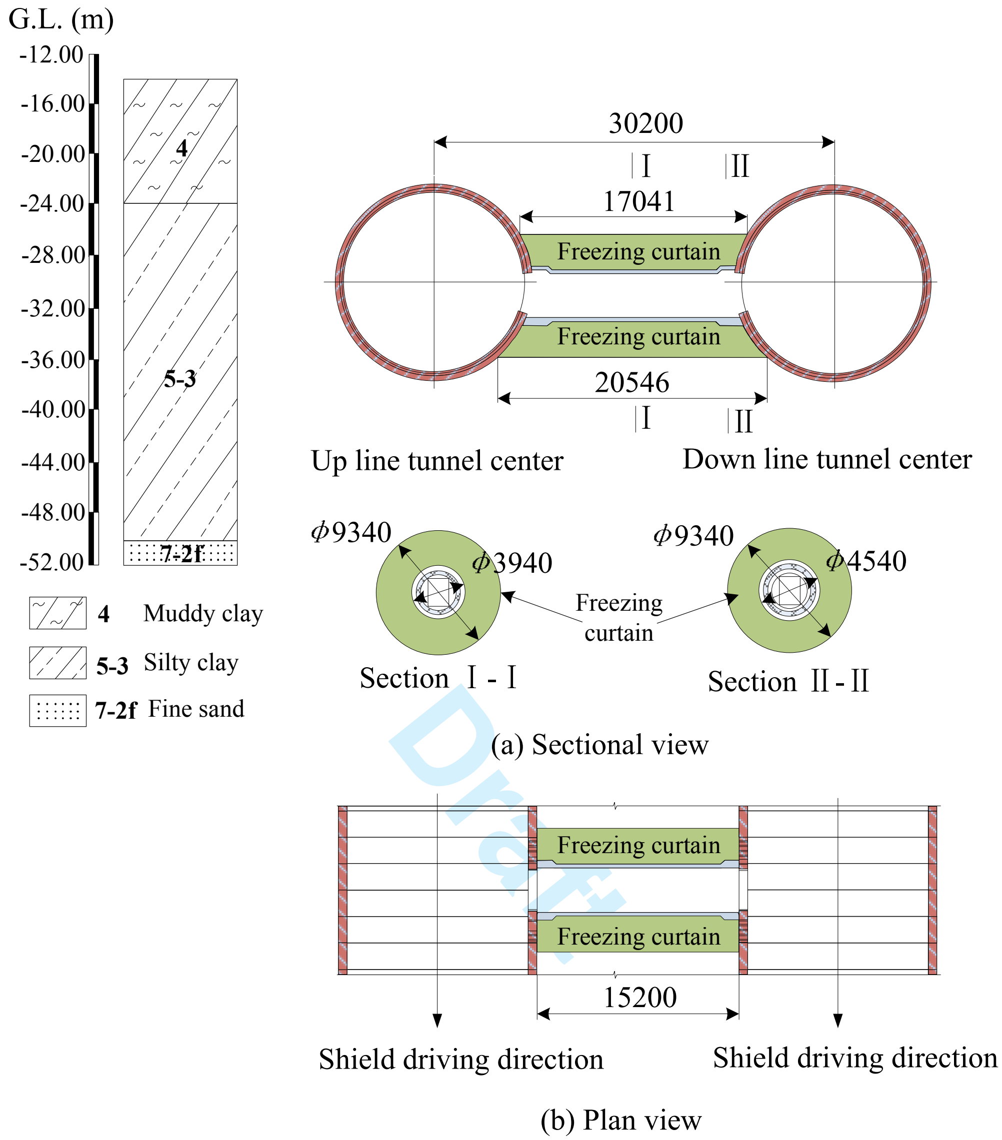

Fig. 3. Sectional and plan view of cross passage for Shanghai Yangtze River Tunnel

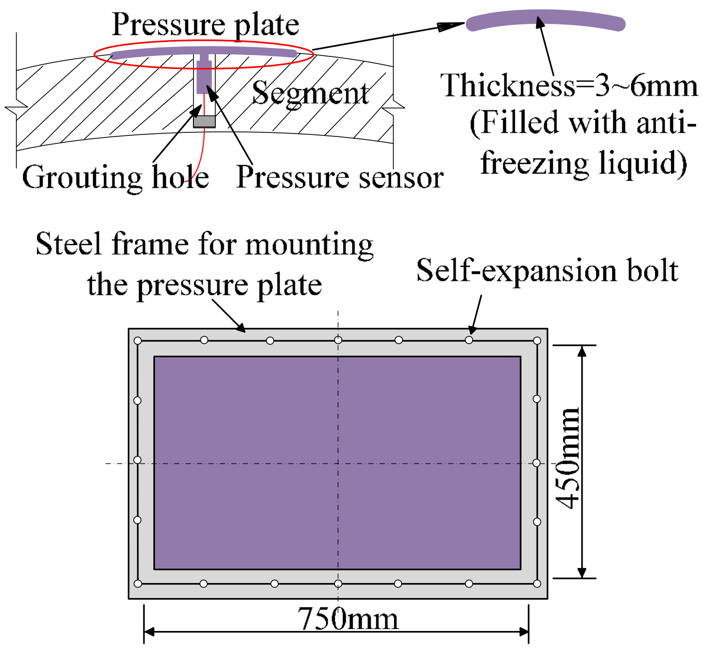

Fig. 4. Installation method of pad-type earth pressure gauge

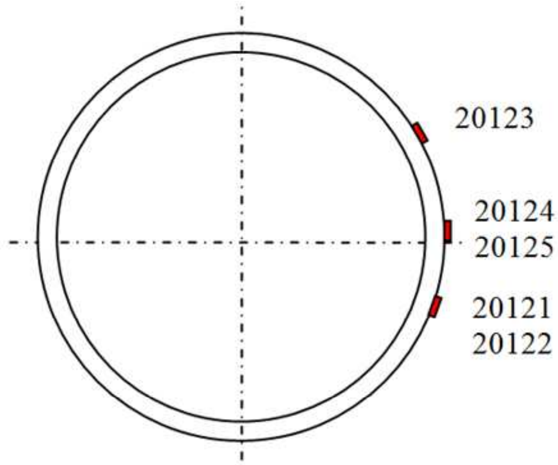

a) Sectional view

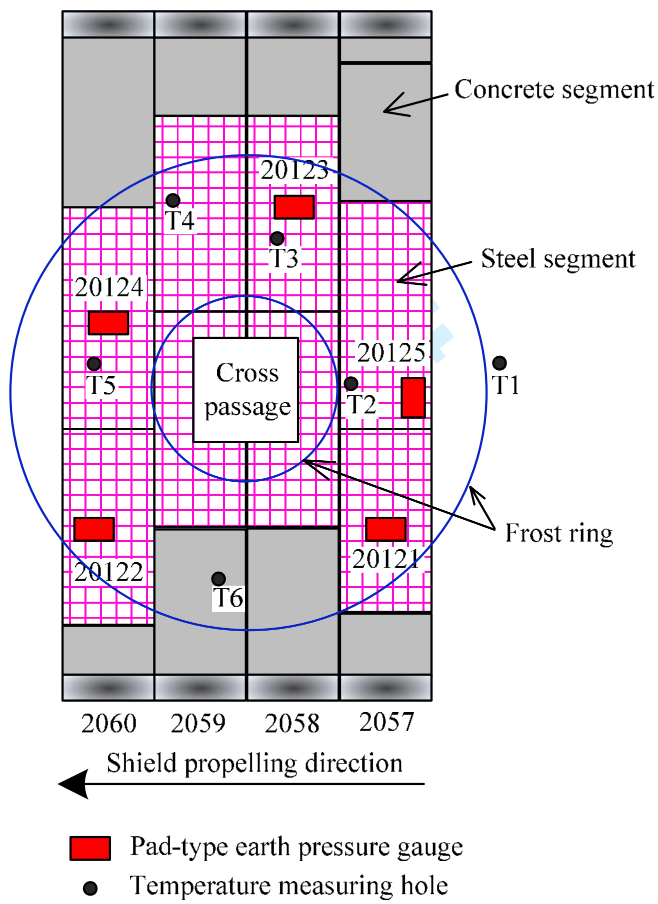

b) Plan view

Fig. 5. Installation positions of 5 pad-type earth pressure gauges and temperature measuring holes

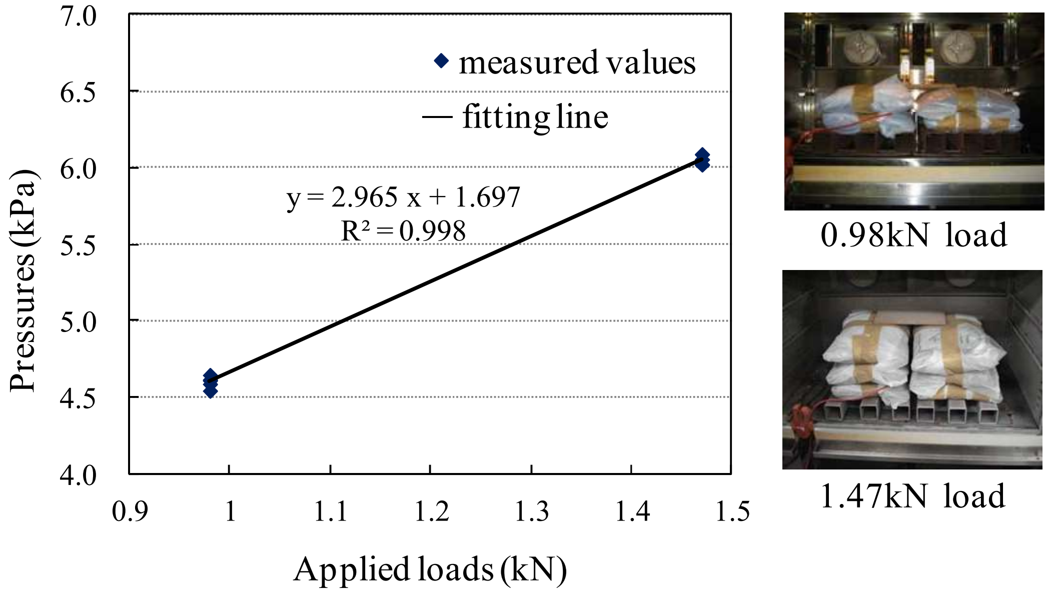

Fig. 6. Relationship between measured pressures and applied loads at the temperature of -35°C

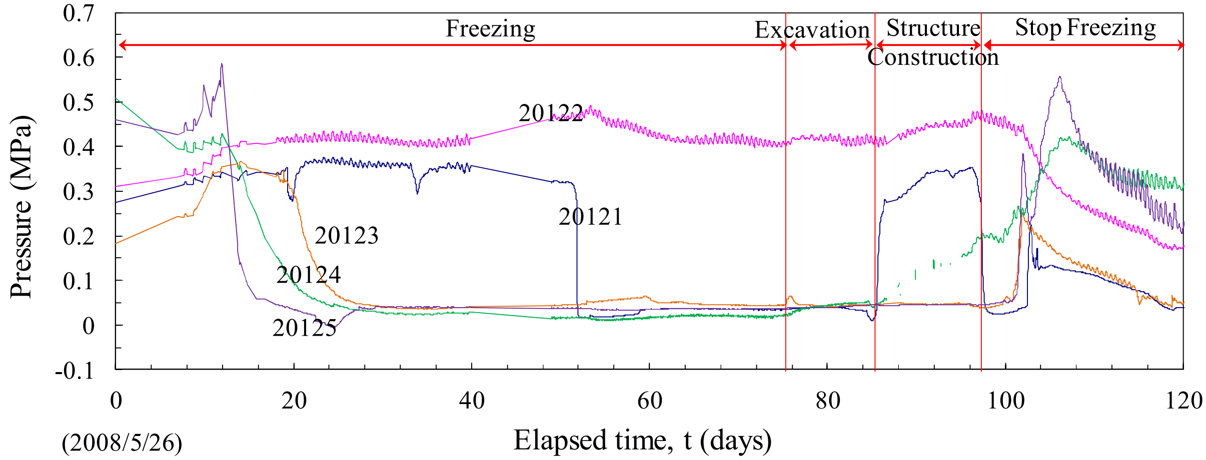

(a) Earth pressures

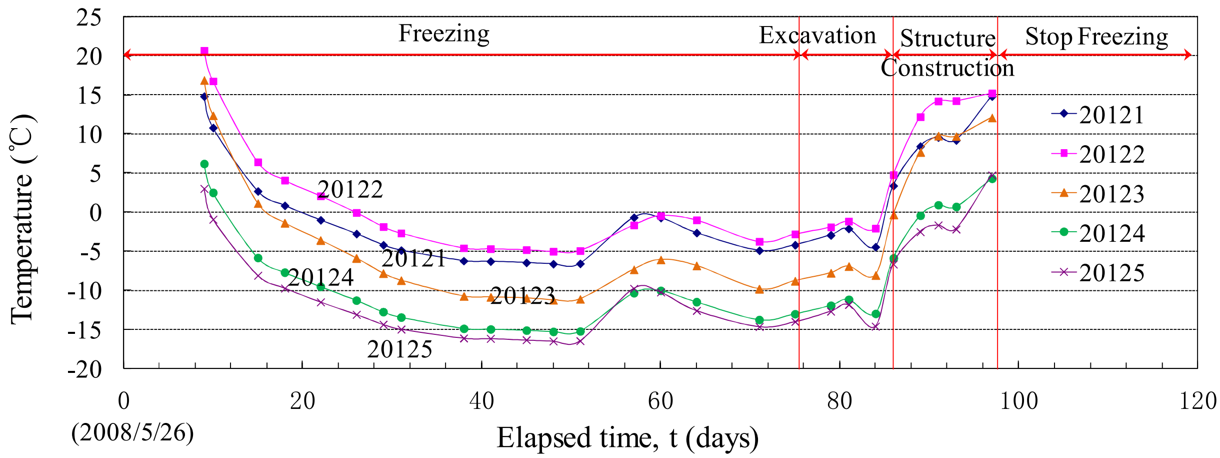

(b) Temperatures

Fig. 7. Timeline of measured earth pressures and temperatures

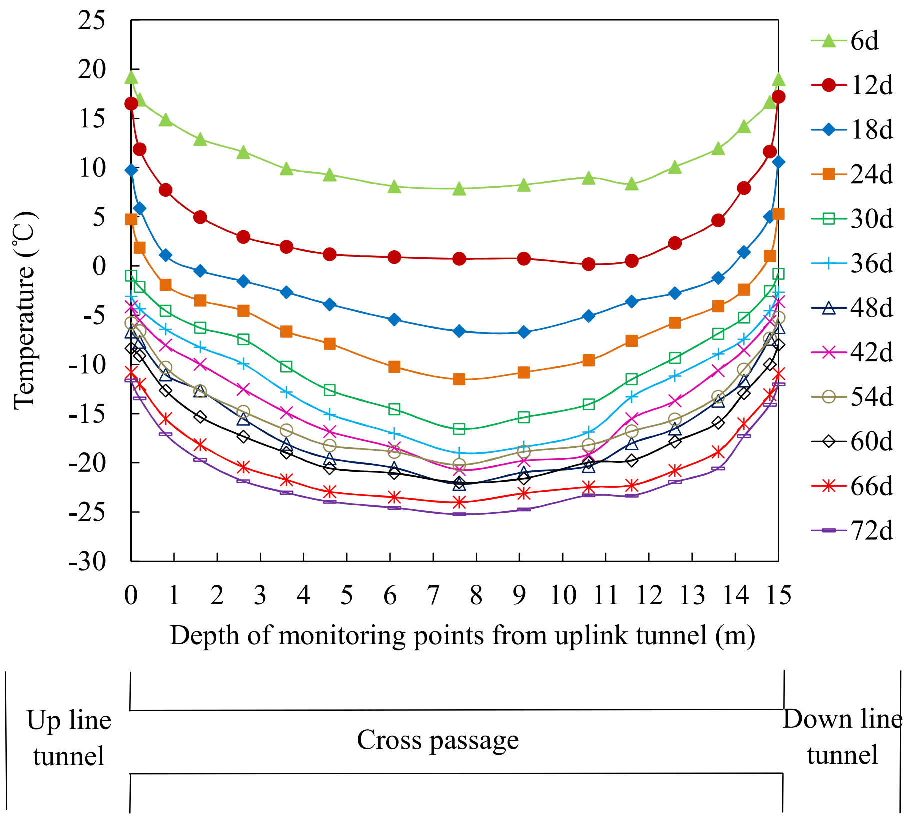

Fig. 8. Temperature distribution along T2 measuring hole at different times during the freezing process

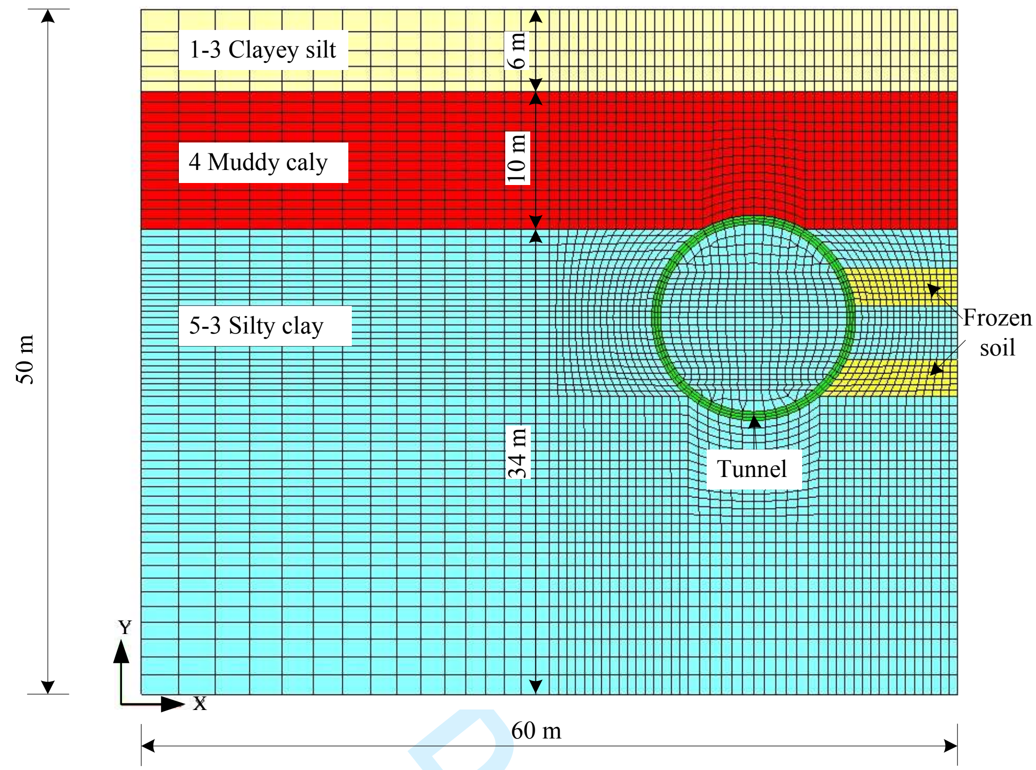

Fig. 9. FEM model for analysing the drop-down of frost heave pressure during freezing

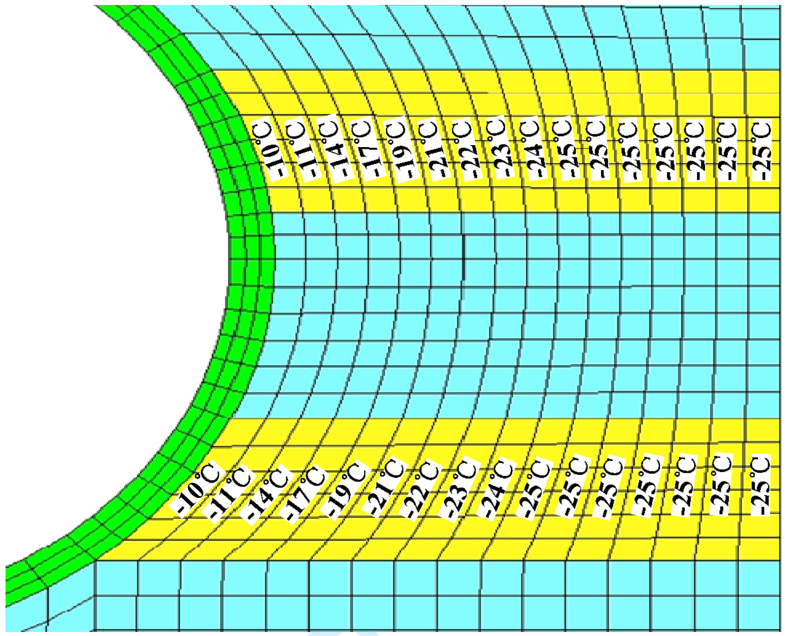

Fig. 10. Prescribed final temperatures in the frozen ring, used for thermal-mechanical coupled analysis

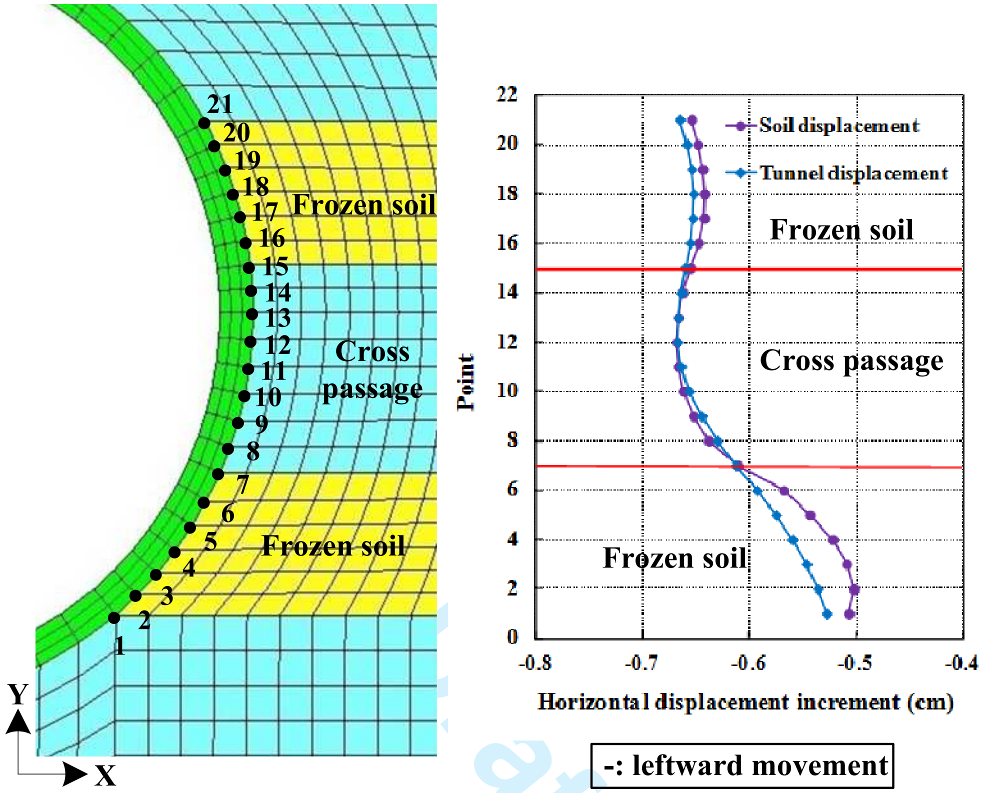

Fig. 11. Horizontal displacement increment of tunnel and soil in frozen zone between before and after freezing

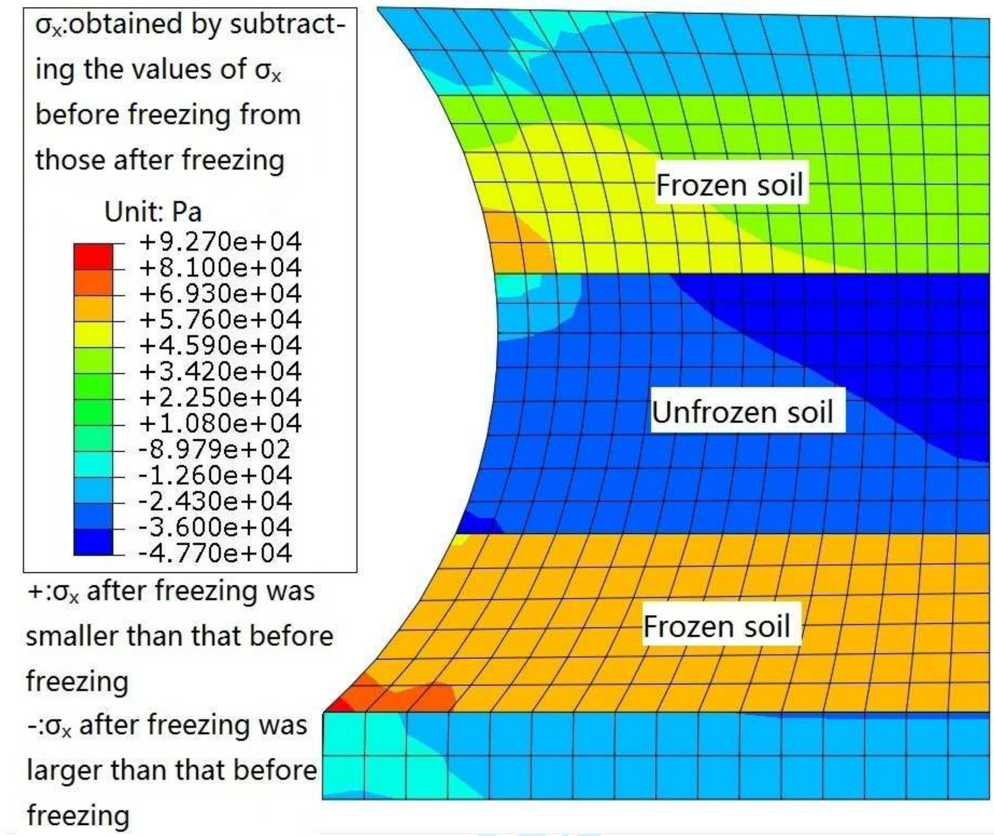

Fig. 12. Distribution of σ_x, obtained by subtracting the values of σ_x before freezing from those after freezing

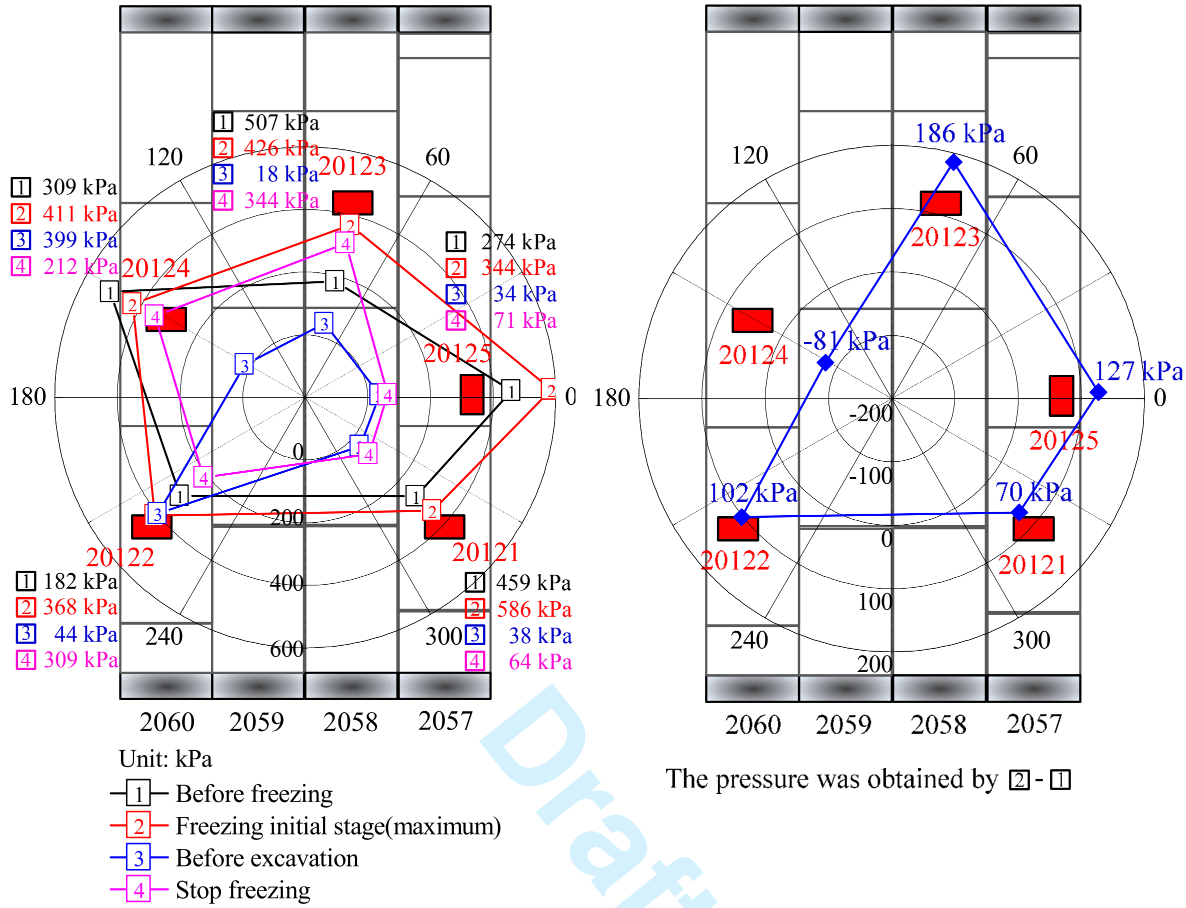

(a) Distribution of frost heave pressures (b) Maximum frost heave pressures of 5 measuring points

Fig. 13. Distribution of measured frost heave pressures upon the tunnel

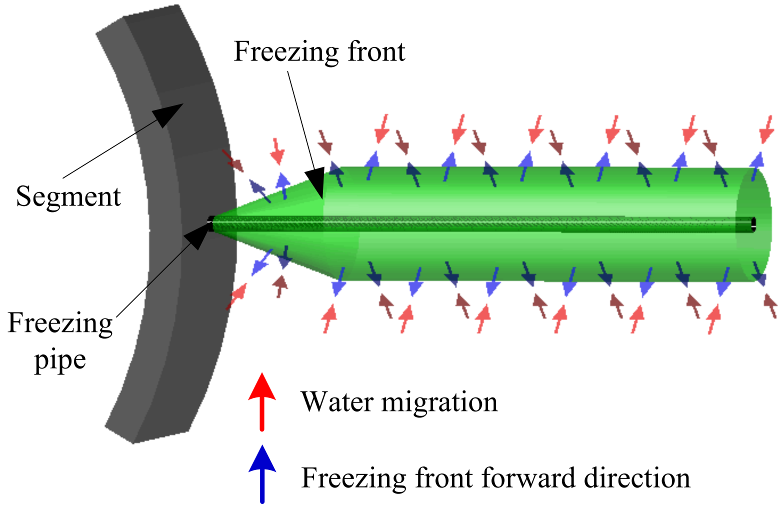

Fig. 14. Illustration of water migration in the early stage of freezing.

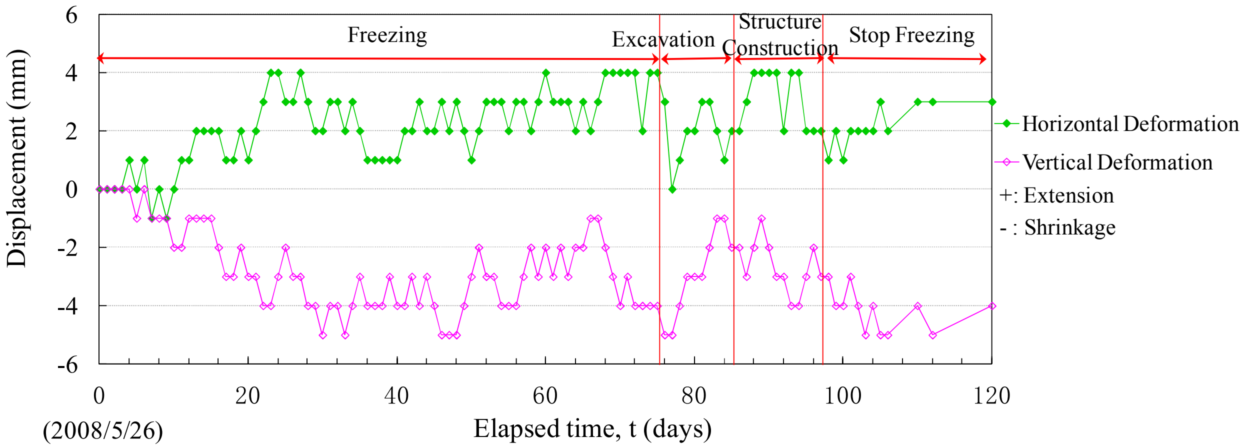

Fig. 15. Timeline of cross-sectional deformation of up line tunnel

Photo 1. Excavation of cross passage for Shanghai Yangtze River Tunnel by the mining method

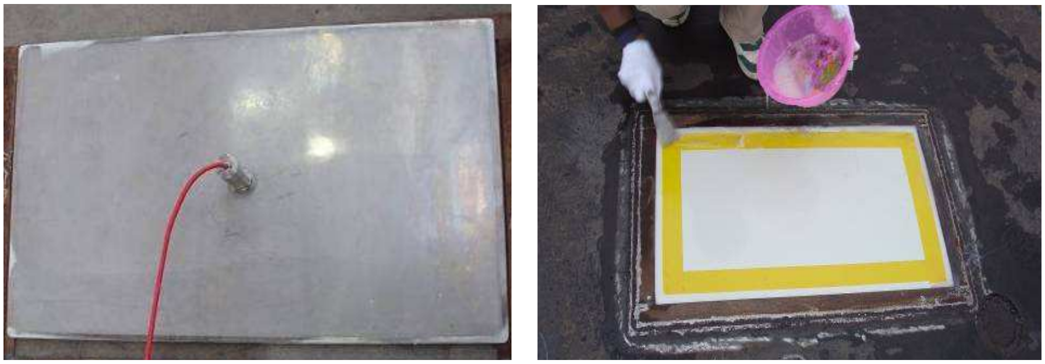

a) Before installation b) After installation

Photo 2. Photos of earth pressure gauge before and after installation

Photo 3. Photo taken in front of steel segments at the start of freezing